Zootaxa 5839 (3): 563–576
https://www.mapress.com/zt/

Article

ISSN 1175-5326 (print edition)
ZOOTAXA
ISSN 1175-5334 (online edition)

https://doi.org/10.11646/zootaxa.5839.3.8
http://zoobank.org/urn:lsid:zoobank.org:pub:A8FC4D51-7DF2-4A46-ADC9-CD059C995193

A new species of the genus *Dysommina* (Teleostei: Anguilliformes: Synaphobranchidae) from the eastern South Atlantic Ocean off Angola

KENNETH A. TIGHE
Department of Vertebrate Zoology, National Museum of Natural History, Smithsonian Institution, Museum Support Center, MRC 534, 4210 Silver Hill Road, Suitland, MD 20746, USA
tighek@si.edu; https://orcid.org/0000-0003-1127-0949

Abstract

Dysommina castanea **sp. nov.**, a species of ilyophine eel from the eastern South Atlantic Ocean off Angola is described and illustrated. The species is distinguished from the other four species in the genus, *D. rugosa*, *D. orientalis*, *D. brevis* and *D. pygmaea*, by a combination of morphometric and meristic characters, dentition and coloration.

Key words: Pisces, Elopomorpha, taxonomy, Angola, South Atlantic, *Dysommina rugosa*

Introduction

The genus *Dysommina* and its only included species, *D. rugosa*, was described by Ginsburg (1951) based on a single specimen (USNM 131594) taken off Cumberland Island, Georgia. Since the original description, *D. rugosa* has been reported to be nearly world-wide in distribution including the western North Atlantic from off the Carolinas to the Gulf of Mexico and the Caribbean Sea (Robins and Robins 1989), off Surinam (Uyeno & Sasaki 1983), off southern Brazil (Haimovici *et al.* 1994), off Angola (Tweddle & Anderson 2008), in the Mozambique Channel (Karrer 1983), Japan (Hatooka 1997), Taiwan (Chen & Mok 2001; Ho *et al.* 2015), Vailulu'u Seamount, American Samoa (Staudigel *et al.* 2006) and Hawaii (Robins & Robins 1976). Tighe *et al.* (2018) described a new species, *Dysommina orientalis*, based on the specimens previously reported as *Dysommina rugosa* from Taiwan and Japan. Recently, Vo *et al.* (2024) described a new species, *Dysommina brevis,* from the South China Sea off Vietnam, and Tighe & Pogonoski (2025) described a new species, *Dysommina pygmaea,* from the eastern Indian Ocean off Western Australia. Reexamination of the specimen reported from the eastern South Atlantic Ocean off Angola by Tweddle & Anderson (2008) found it to be an undescribed species in this genus which is described below.

Materials and methods

General methods for morphometric and meristic data for this study are given in Böhlke (1989). Measurements over 100 mm were made with a 450 mm ruler to the nearest 1 mm and measurements between 10–100 mm were made with a digital caliper to the nearest 0.1 mm. Measurements under 10 mm which were taken with an ocular micrometer. All measurements are given as a proportion of the total length (TL) except for subunits of the head which are presented as proportions of the head length (HL). Vertebral and fin ray counts were taken from radiographs. Total vertebral counts are of all elements including the hypural plate. Preanal and predorsal vertebral counts were taken using the definitions of Böhlke (1982). The number of dorsal rays anterior to the anal origin are counted back to the vertical through the first anal ray base. Cyanine blue was used for staining cephalic sensory pores (Saruwatari *et al.*, 1997). The holotype was scanned on a GE Phoenix v|tome|x M 240/180kV Dual Tube µCT scanner at the Micro Computed Tomography Imaging Center (mCTIC) at the Smithsonian Institution National Museum of Natural History Scientific Imaging Core Facility (RRID:SCR_025090) with the following settings: 115 kV, 125

Accepted by G. Short: 2 May 2026; published: 30 Jun. 2026

μA, 250 ms exposure time, and 18.006334 μm voxel size. The resulting x-ray projections were reconstructed into three-dimensional image stack using the software package datos|x reconstruction vers. 2.4.0, and were visualized and segmented using 3D Slicer vers. 5.6.2 (Fedorov *et al.*, 2012). The resulting three-dimensional image stack was uploaded to MorphoSource (media identification number 000772053). The specimen is deposited at the South African Institute for Aquatic Biodiversity (SAIAB). Other institutional codes used follow Sabaj (2020; 2025)

***Dysommina castanea* sp. nov.**
Figures 1–14, Table 1

Holotype: SAIAB 66023 (358 mm TL); Eastern South Atlantic Ocean: off Angola, 09° 53’ S, 12° 39’ E, RV Dr Fridtjof Nansen, Station 2764, depth 536–542 m, 10 March 2002.

FIGURE 1. Holotype of *Dysommina castanea***,** SAIAB 66023 (358 mm TL); Eastern South Atlantic Ocean: off Angola.

Diagnosis. A species of the genus *Dysommina* with the following combination of characters: predorsal vertebrae 13, preanal vertebrae 26, total vertebrae 134, eye diameter around 10% head length, vomerine dentition consisting of 4 large compound teeth set in papillose pads with a fifth small tooth more posteriorly, maxillary and dentary teeth less numerous and small, total of 7 POM pores with the last located posterior to the jaw rictus, body coloration dark brown.

Description. Body moderately elongate, slightly compressed in head and trunk. Pectoral fin present; dorsal-fin origin over tip of pectoral fin; anal fin origin approximately one head length behind pectoral fin base. Snout projects slightly beyond tip of lower jaw. Snout plicate, with four main plicae on each side of mid-line; first and third plicae unite anteriorly into a U shape, surrounding second plica; fourth plica smaller and less distinct than others; first supraorbital pore just above dorsal end of second and third plicae. Tip of lower jaw also plicate, with total of 11 plicae; median plica largest and slightly pigmented; five unpigmented lateral plicae on each side of median plica, reducing slightly in size from interior to exterior with outermost much smaller and indistinct; first preopercular-mandibular pore just behind posterior end of third and fourth plicae. Anterior portion of snout and lower jaw extensively covered with papillae and leaf-shaped skin flaps; skin flaps gradually reduced in size and number posteriorly. Papillae also reduce in number posteriorly along head. Upper and lower lips with three rows of hair-like sensory papillae.

Morphometrics: total length (TL) 358 mm; predorsal length 62.1 mm (17.3 % TL); preanus length 90.0 (25.1 % TL); preanal length 100.0 mm (27.9 % TL); body depth at gill opening 19.8 mm (5.5 % TL); body width at gill opening 11.1 mm (3.1 % TL); body depth at anus 20.6 mm (5.8 % TL); body width at anus 12.1 mm (3.4 % TL); head length (HL) 50.9 mm (14.2 % TL); eye diameter 5.6 mm (11.0 % HL); interorbital width 7.0 mm (13.8 % HL); snout length 14.8 mm (29.1 % HL); upper jaw length 20.7 mm (40.7 % HL); lower jaw length 19.5 mm (38.3 % HL); gill opening 6.3 mm (12.4 % HL); interbranchial width 5.0 mm (9.8 % HL).

Meristics: total vertebrae 134; predorsal vertebrae 13; preanal vertebrae 26; dorsal rays 314; anal rays 292; anal fin origin at dorsal ray 38; pectoral rays 16; caudal rays 15.

Coloration: Body uniformly dark brown; dorsal and anal fins with light margins anteriorly, becoming dark in posterior one third of tail (Fig. 1). Head grayish brown; lower jaw grayish with light speckles; pectoral fin light gray (Fig. 2A).

FIGURE 2. A. Head of holotype of *Dysommina castanea*, SAIAB 66023. B. Drawing of head of SAIAB 66023 showing cephalic lateralis pores. Arrows show dorsal fin origin.

FIGURE 3. MicroCT scan of the skull of *Dysommina castanea*, SAIAB 66023. A. Ventral view showing the vomerine and maxillary dentition. B. Dorsal view showing the dentary dentition. Abbreviations: AR, angulo-articulo-retroarticular; BO, basioccipital; CM, coronomeckelian ossification; DE, dentary; EV. Ethmovomerine complex; EX, exoccipital; FR, frontal; MX, naxillary; PR, prootic; PS, parasphenoid; PT, pterotic; PTS, pterosphenoid; SP, sphenotics.

Cephalic-lateralis pores (Fig. 2B). supraorbital 3; adnasal 1, infraorbital 4, preoperculomandibular 7 (6 along length of mandible and 1 posterior to rictus of jaw). Lateral line pores absent.

Dentition (Fig. 3). Intermaxillary teeth absent. Five relatively large, compound vomerine teeth set in papillose pads, fifth slightly smaller than the first four teeth on the palate. However, the second and third vomerine teeth are set in a single socket (Fig. 3A). The anterior of the two teeth is cracked and the back of the root is missing (Fig. 6B). These two teeth may be an original tooth and a replacement tooth that started growing when the original tooth was damaged. The fourth vomerine tooth is complete but shows a small replacement tooth embedded in the tissue just anterior to the tooth. Dentary teeth set in a band composed of 4–5 irregular rows anteriorly and decreasing gradually to 3–4 rows posteriorly, teeth increasing in size gradually from outer to inner with approximately 30–33 teeth in inner row. Maxillary teeth similar but set in a band composed of 4–5 irregular rows anteriorly and decreasing gradually to 2–3 rows posteriorly, teeth increasing in size gradually from outer to inner row with approximately 36–37 teeth in inner row.

Osteology (Fig.4). The osteology of *Dysommina castanea* is nearly identical to that of *D. rugosa* described by Robins and Robins (1970) and that of *D. pygmaea* described by Tighe and Pogonoski (2025). Fig. 4 shows the osteology of the head of D. *castanea* in dorsal, lateral and ventral views. Details of the osteology are discussed individually in the sections below.

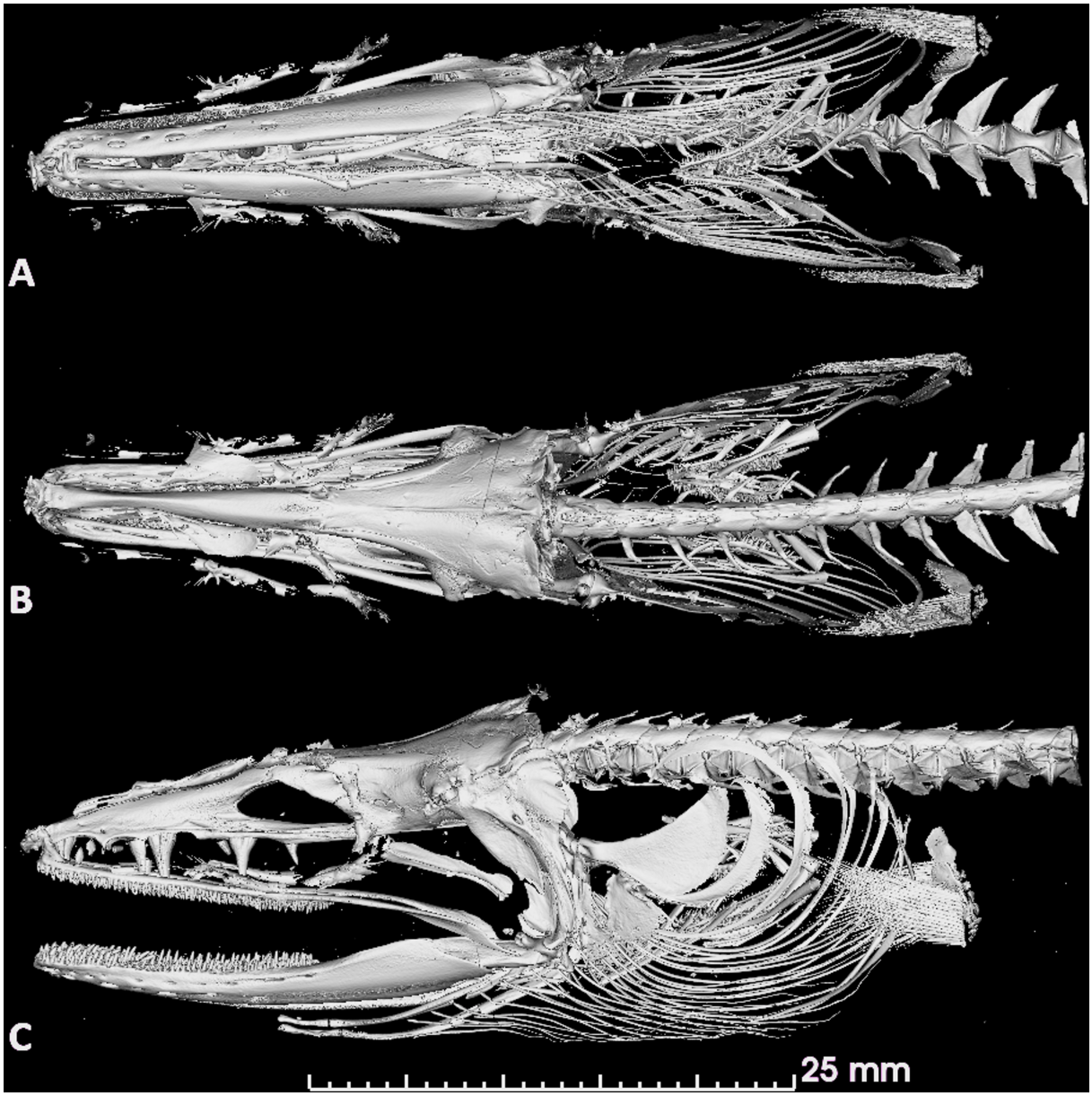

FIGURE 4. MicroCT scan of the anterior portion of the holotype of *Dysommina castanea***,** SAIAB 66023. A. Ventral view. B. Dorsal view. C. Lateral view.

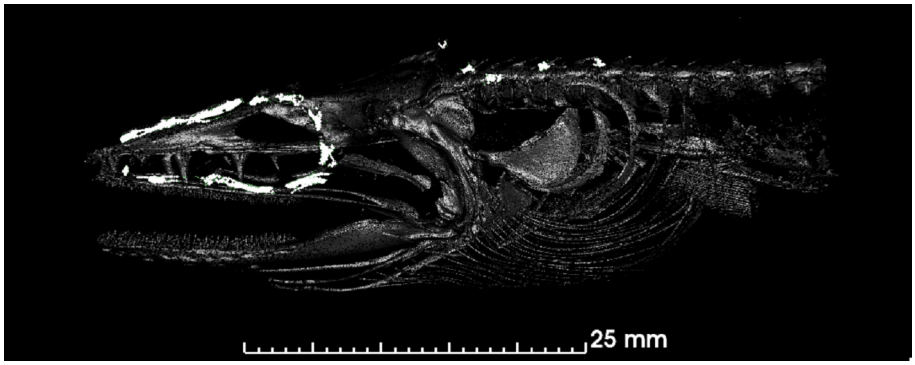

FIGURE 5. MicroCT scan of the anterior portion of the holotype of *Dysommina castanea***,** SAIAB 66023 showing cephalic and lateral line ossicles (white blotch-like areas).

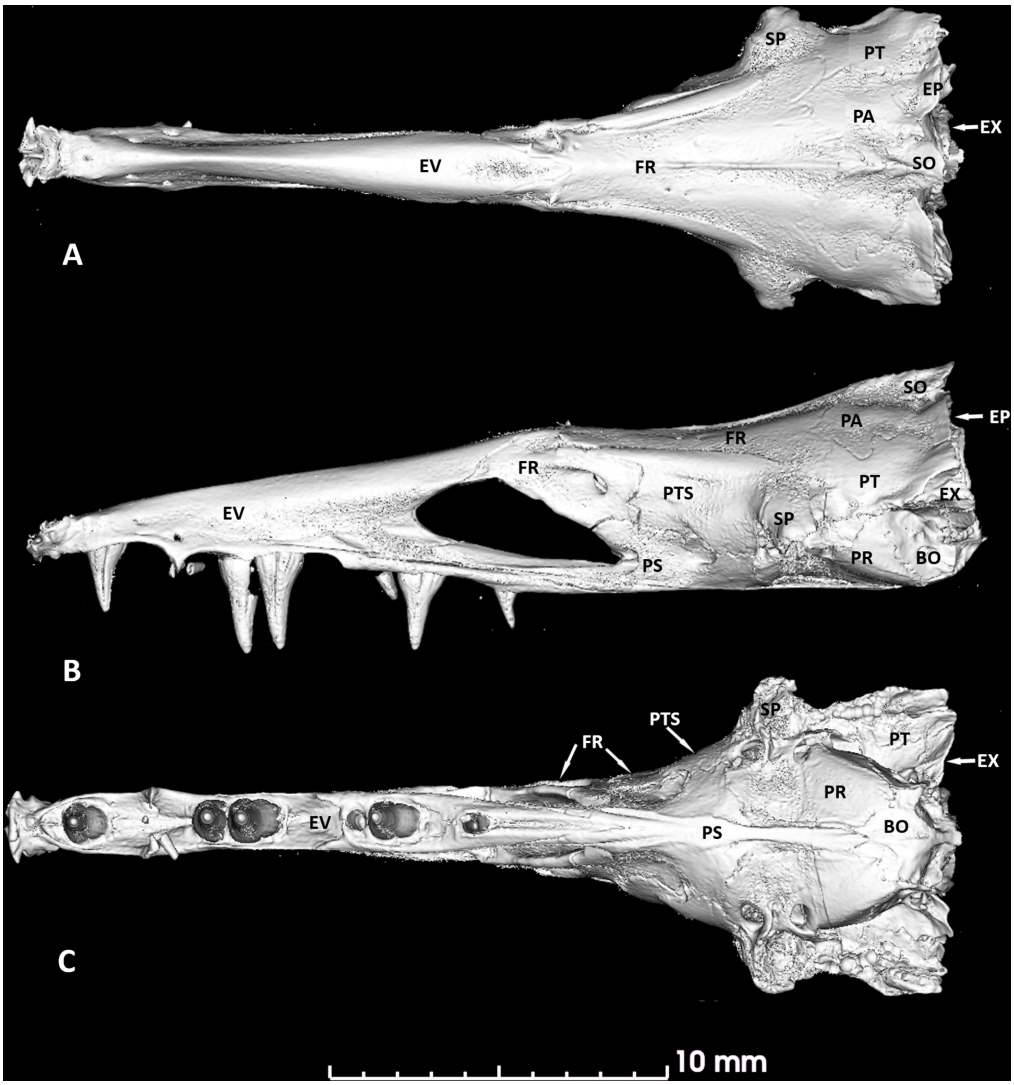

FIGURE 6. MicroCT scan of the neurocranium of the holotype of *Dysommina castanea***,** SAIAB 66023. A. Dorsal view. B. Lateral view. C. Ventral view. Abbreviations: BO, basioccipital; EP, epiotic; EV. Ethmovomerine complex; EX, exoccipital; FR, frontal; PA, parietal; PR, prootic; PS, parasphenoid; PTS, pterosphenoid; PT, pterotic; SO, supraoccipital; SP, sphenotic.

Cephalic lateralis (Fig. 5). There are 9 cephalic-lateralis ossicles on the dorsal surface of the head, posterior to the eye and along the upper jaw. The anteriormost on the dorsal surface is the nasal ossicle which supports the dorsal portion of the nasal chamber. There are two small ossicles along the portion of the supraorbital canal above the eye

and two ossicles on the postocular portion of the infraorbital canal, but there are no pores associated with them. There are five ossicles associated with the infraorbital canal. The first, anterior most is on the adnasal branch of the infraorbital and the adnasal pore is near its distal end. The first infraorbital pore is anterior to the next infraorbital ossicle, near the junction of the adnasal branch with the main infraorbital canal. The second infraorbital pore is between the second and third infraorbital ossicles. The third infraorbital pore is posterior to the third infraorbital ossicle, and the final infraorbital pore is anterior to the fifth infraorbital ossicle. Despite the lack of lateral line pores, there are 5 very small lateral-line ossicles in the supratemporal and branchial anterior portion of the lateralis nerve as there are superficial sensory papillae along the region of the lateral line despite the lack of open pores.

Neurocranium (Fig. 6). The skull of *D. castanea* is completely ossified with little cartilage and shows a generalized anguilliform pattern with the fused ethmovomer. The frontals are fused and cover nearly half of the dorsal surface of the skull. The remainder of the dorsal surface of the skull is composed of the paired parietals, pterotics, epiotics, sphenotics and the single, median supraoccipital. The ventral portion of the skull is composed of the fused ethmovomer, the parasphenoid, the prootics, the exoccipitals and the basioccipital. In addition, the lateral portions of the pterosphenoids, pterootics and sphenotics are visible in the ventral view. The dorsal portion of the orbit is formed primarily by the frontal. The ethmovomer forms the anterior margin of the orbit while the ventral and posterior margins are formed primarily by the parasphenoid. Robins and Robins (1970) reported that the basisphenoid and parasphenoid are fused in *D. rugosa*, and this is probably the same in *D. castanea* as there is no autogenous basisphenoid visible on the scan.

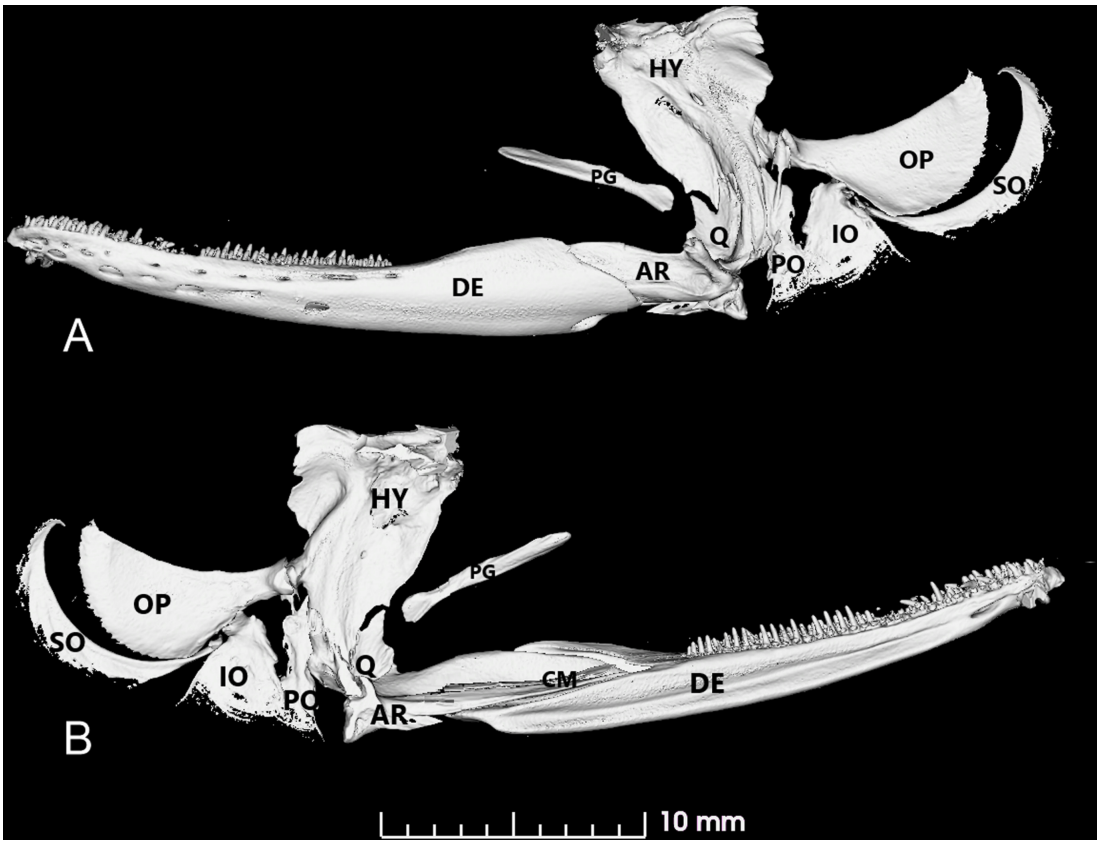

FIGURE 7. MicroCT scan of the left suspensorium, opercular series and lower jaw of holotype of *Dysommina castanea***,** SAIAB 66023. A. Lateral view. B. Medial view. Abbreviations: AR, angulo-articulo-retroarticular; CM, coronomeckelian ossification; DE, dentary; HY, hyomandibular; IO, interopercle; OP, opercle;PO, preopercle; Q, quadrate; SO, subopercle.

Suspensorium (Fig. 7). The hyomandibular is inclined slightly posteriorly and articulates with the neurocranium anteriorly with a hemispherical "ball and socket" joint underneath the sphenotic and posteriorly in a groove along the ventral surface of the pterotic. The hyomandibular and quadrate articulate in a complex interdigitated suture. Ventrally, the quadrate ends in a broad rounded concave process that articulates with a saddle-shaped surface at the proximal end of the angulo-articulo-retroarticular of the mandible. The angulo-articulo-retroarticular narrows

anteriorly into a trough-shaped projection which inserts into the hollow proximal end of the dentary. The ossification of the coronomeckelian lies within this U-shaped inner surface of the angulo-articulo-retroarticular. The pterygoid is relatively stout but does not articulate the hyomandibular or quadrate. It is embedded within connective tissue or muscle and extends to near the posterior end of the maxilla. The opercular series is complete with all four elements present although greatly reduced in ossification especially along the margins. The opercle articulates with the hyomandibular through a bottle-neck articular condyle. The subopercle has an anterior condyle that seems to articulate with a socket on the interopercle although the bones do not actually touch in the scan. The subopercle

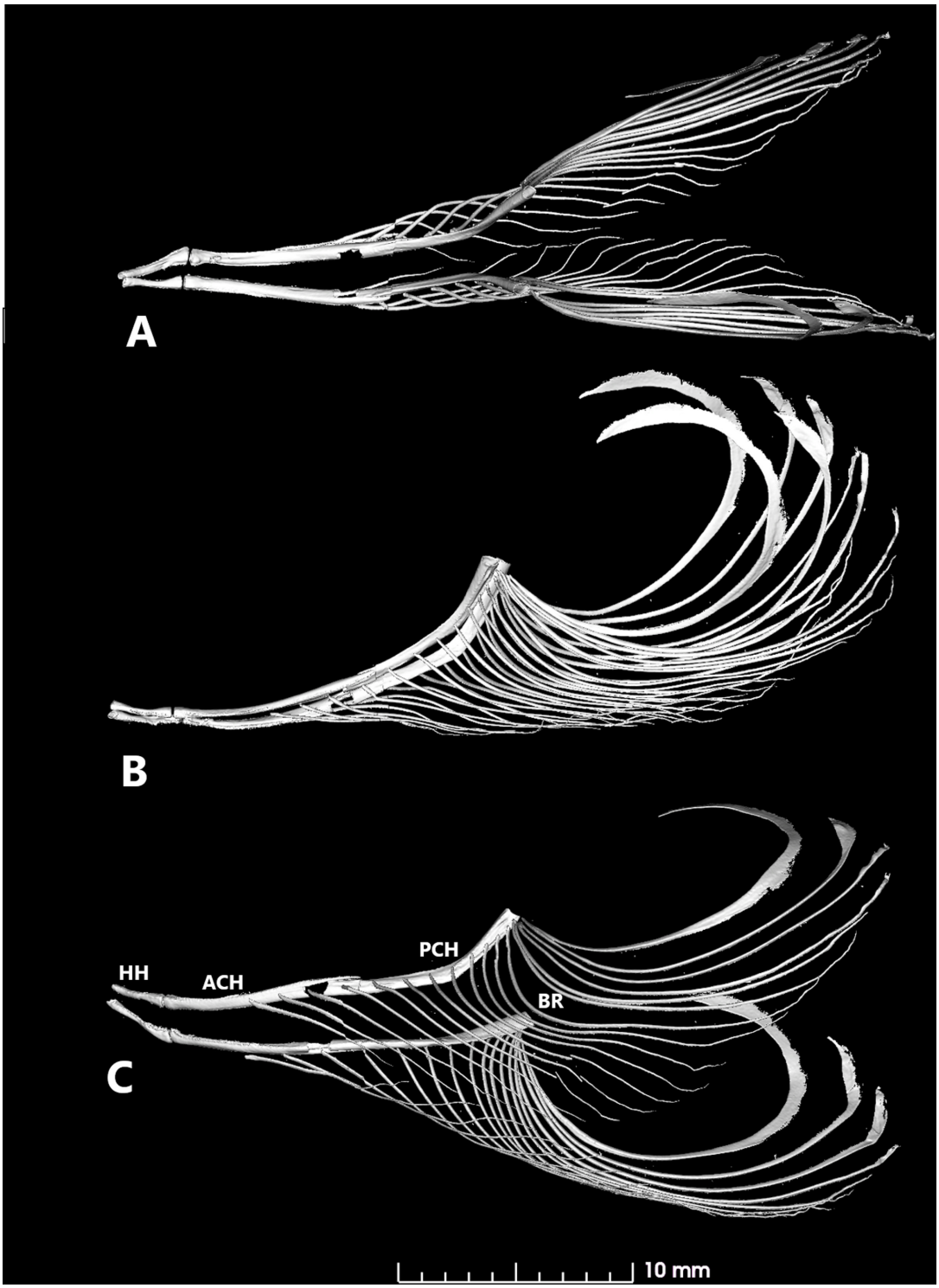

FIGURE 8. MicroCT scan of the hyoid arches of holotype of *Dysommina castanea*, SAIAB 66023. A. Dorsal view. B. Lateral view C. Ventro-lateral view. Abbreviations: ACH, anterior ceratohyal; BR, branchiostegal rays; HH, hypohyal; PCH, posterior ceratohyal.

becomes more laterally flattened posteriorly and curves around the ventral margin of the opercle. The preopercle lies along the posterior margin of the hyomandibular and is slightly tube-like to house the preopercular branch of the cephalic lateralis. There is a dorsal extension of the preopercle which ends in what looks like a cephalic lateral line ossicle which probably supports the preopercular canal. The interopercle is a quadrilateral-shaped bone that is ventral and medial to the rest of the opercular series. There are two small dorsal projections which fall on either side of the ventral edge of the opercle.

Hyoid arch (Fig. 8). The ossified elements of the hyoid arch include paired hypohyals, anterior ceratohyals and posterior ceratohyals. The hypohyals are small tapered cylindrical bones and are articulated to the anterior tip of the anterior ceratohyals. The anterior ceratohyals are also cylindrical with a narrow splint of bone extending onto the dorsal surface of the posterior ceratohyals. The posterior ceratohyals are cylindrical anteriorly but become laterally flattened and curve dorsally posteriorly. There are 17–18 branchiostegal rays. The first and second branchiostegals originate near the end of the anterior ceratohyal, the third on the interspace between the anterior and posterior ceratohyals, and the rest on the posterior ceratohyal. The last branchiostegal is laterally flattened for approximately half of its length and curves up and around the opercle posteriorly, nearly closing a circle. The next one or two branchiostegals also have their tips laterally flattened but do not curve as far forward around the opercle.

Pectoral fin (Fig. 9). The CT scan of the pectoral girdle shows the following ossified elements: cleithrum, coracoid, scapula, four actinosts and 16 fin rays.

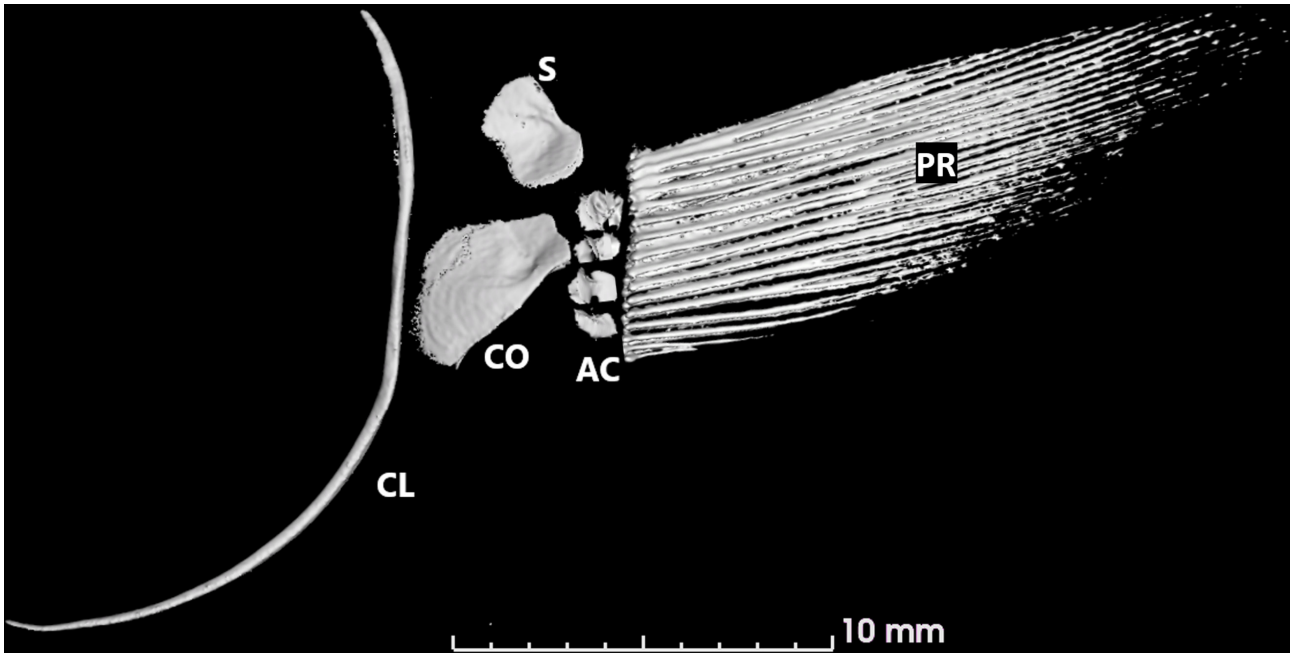

FIGURE 9. MicroCT scan of the left pectoral fin of holotype of *Dysommina castanea***,** SAIAB 66023. Lateral view. Abbreviations: AC, actinosts; CL, cleithrum; CO, coracoid; PR, pectoral rays; S, scapula.

Branchial arches (Fig. 10). Bones of the gill arches are the following: two pairs of hypobranchials, five pairs of ceratobranchials, four pairs of epibranchials, one pair of infrapharyngobranchials and two pairs of pharyngobranchial toothplates. Both lower and upper pharyngobranchial toothplates are roughly ovoid and covered with small, conical teeth. Robins and Robins (1970) reported that, in *D. rugosa*, there were two pairs of infrapharyngobranchials and that both lower and upper pharyngobranchial toothplates are single bones. In *D. castanea*, there is only a single pair of infrapharyngobranchials. In addition, the upper pharyngobranchial toothplates consist of two bones. The main bone of the toothplate is the upper pharyngobranchial 4 which is the largest and completely toothed. Anterior to this bone is a small elongate, sub-triangular bone (upper pharyngobranchial 3) which is closely associated (and possibly partially fused) with infrapharyngobranchial 3.

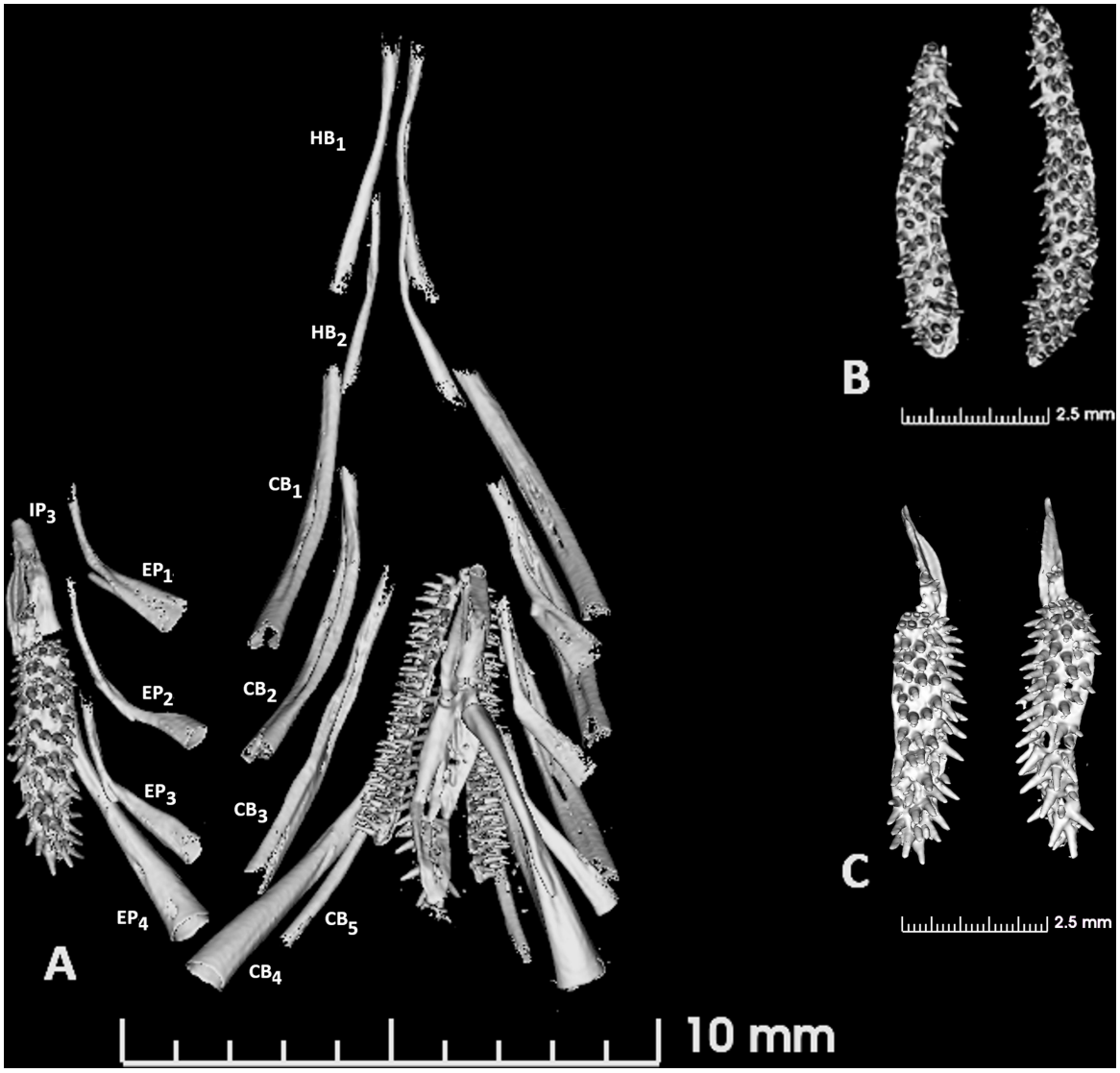

FIGURE 10. MicroCT scan of the branchial arches of holotype of *Dysommina castanea***,** SAIAB 66023. A. Branchial arches in dorsal view, with upper elements of left branchial arch flipped to allow ventral view. B. Lower pharyngeal toothplates. C. Upper pharyngeal toothplates. Abbreviations: CB, ceratobranchial; EP, epibranchial; HB, hyobranchial; IP, infrapharyngobranchial.

Comparative remarks. *Dysommina castanea* is very similar in meristics to the other described species of *Dysommina* (Table 1). The predorsal vertebral number (13) is within the range of all other species except *D. orientalis* (11–12) and *D. pygmaea* (16). The preanal vertebral number (26) is lower than the range of the other species except *D. orientalis* (26–32) and *D. brevis* (23, 25). The total vertebral count (134) is higher than the other species except *D. brevis* (133, 134). The number of dorsal rays (314) is within the range of *D. rugosa* (286–339) and *D. orientalis* (304–321), but less than the range in *D. brevis* (338, 344) and greater than the range of *D. pygmaea* (271–300). The number of anal rays (292) is greater than the range of *D.rugosa* (258–276), *D. orientalis* (260–289) and *D. pygmaea* (258–276), but less than the range in *D. brevis* (304, 309). The number of dorsal rays anterior to the anal origin (38) is within the range of *D. rugosa* (36–57) but less than the range in *D. orientalis* (51–60) and *D. brevis* (42, 41) and greater than the range of *D. pygmaea* (29–34).

Dysommina castanea is also very similar in morphometrics to the other described species of *Dysommina* (Table 1). Predorsal length (17.3% TL) is within the range of all other species except *D. orientalis* (14.0–16.2) and *D. pygmaea* (20.7–21.7). Preanal length (27.9% TL) is within the range of all other species except *D. brevis* (24.6, 25.6). Tail length (72.1% TL), as the reciprocal of preanal length, is also within the range of all other species

TABLE 1. Morphometric and meristic data of *Dysommina castanea, Dysommina rugosa, Dysommina orientalis, Dysommina brevis* and *Dysommina pygmaea*.

	D. castanea	*D. rugosa*	*D. orientalis*	*D. brevis*[*]	*D. pygmaea*
	Holotype	Study Material	Study Material	Holotype, Paratype	Type series
Total length (mm)	358	96–347 (n=54)	238–625 (n=7)	319, 282	145–169 (n=4)
% TL		Mean (range)	Mean (range)		Mean (range)
Predorsal length	17.3	18.4 (15.3–21.1)	15.0 (14.0–16.2)	17.0, 17.7	21.3 (20.7–21.7)
Preanal length	27.9	28.90 (26.1–32.0)	28.7 (27.0–29.8)	24.6, 25.6	28.9 (27.2–29.7)
Tail length	72.1	70.9 (68.0–73.9)	71.3 (70.2–73.0)	75.4, 74.4	71.0 (69.0–73.7)
Trunk length	13.7	14.9 (11.7–17.2)	15.8 (14.2–17.6)	11.1, 11.8	14.2 (13.0–15.2)
Head length	14.2	14.1(13.0–16.6)	13.2 (12.6–15.0)	13.5, 13.8	14.2 (13.6–14.9)
Depth at gill opening	5.5	5.6 (4.3–7.5)	5.2 (4.9–5.3)	5.7, 5.0	6.6 (6.2–6.7)
Depth at anus	5.8	5.6 (3.9–7.5)	4.7 (3.7–5.9)	5.9, 4.7	7.2 (6.0–8.5)
% HL					
Eye diameter	11.0	11.4 (9.7–15.3)	8.7 (7.6–9.8)	11.8, 12.3	11.8 (9.8–14.3)
Interorbital width	13.8	19.9 (12.6–23.5)	18.5 (17.1–19.5)	17.4, 15.9	16.4 (13.8–20.4)
Snout length	29.1	30.9 (24.6–37.7)	25.3 (23.2–27.8)	28.3, 28.5	28.2 (24.6–33.0)
Upper jaw length	40.7	44.3 (37.6–52.8)	45.9 (43.9–48.0)	43.6, 42.6	42.6 (39.2–47.1)
Lower jaw length	38.3	41.1 (33.3–49.7)	41.3 (39.0–43.4)	38.1, 36.7	40.4 (33.3–44.1)
Pectoral fin length	22.4	17.8 (13.3–23.3)	20.3 (16.8–23.4)	21.3, 18.5	17.7 (13.6–21.7)
Vertebrae					
Predorsal	13	13–16	11–12	12, 13	16
Preanal	26	28–31	26–32	23, 25	27–28
Total	134	123–132	126–132	134, 133	122
Lateralis system					
Cephalic pores					
Supraorbital	3/3	3/3	3/3	3/3, 3/3	3/3
Infraorbital	4/4	5/5	4/4	4/4, 4/4	4/4
Adnasal	1/1	1/1	1/1	0/0, 0/0	1/1
Preoperculomandibular	6+1/6+1	6/6	6/6	6/6, 6/6	6/6
Lateral line	Absent	Absent	Absent	Absent	Absent
Fin rays					
Dorsal-fin rays	314	286–339	304–321	338, 344	271–300
Anal-fin rays	292	258–276	260–289	304, 309	258–276
Anal origin at DR	38	36–57	51–60	42, 41	29–34
Pectoral fin rays	16	13–15		– –, – –	13–15
Caudal fin rays	15				15
Dentition					
Dentary tooth rows	2–5	6–7	5–7	6, 6	5–6
Dentary teeth (inner row)	30–33	ca. 45	41–50	44, 46	28–30
Maxillary tooth rows	3–5	7–8	6–8	5, 4	5–6
Maxillary teeth (inner row)	36–37	ca. 55	50–60	28, 29	37–40
Intermaxillary teeth	0	0	0	0, 0	0
Vomerine teeth	5 large + 1 small	3 large + 1 small	3–4 large + 0–1 small	3 large + 2 small, 4 large + 1 small	4

[*]Data from Vo *et al.* (2024).

except *D. brevis* (75.4, 74.4). Trunk length (13.7% TL) is within the range of *D. rugosa* (11.7–17.2) and *D. pygmaea* (13.0–15.2), but less than the range in *D. orientalis* (14.2–17.6) and greater than *D. brevis* (11.1, 11.8). Head length (14.2% TL) is within the range of all other species except *D. brevis* (13.5, 13.8). Body depth at gill opening and body depth at anus are very similar for all described species of *Dysommina*. These measurements are highly variable and do not provide any diagnostic proportions.

Morphometrics of *Dysommina castanea* based on measurements of elements of the head are also very similar to the other described species of *Dysommina* (Table 1). Eye diameter (11.0% HL) is within the range of *D. rugosa* (9.7–15.3) and *D. pygmaea* (9.8–14.3), but slightly larger than *D. orientalis* (7.6–9.8) and slightly smaller than *D. brevis* (11.8, 12.3). Interorbital width (13.8% HL) is within the range of *D. rugosa* (12.6–23.5) and *D. pygmaea* (13.8–20.4), but slightly smaller than *D. orientalis* (17.1–19.5) and *D. brevis* (17.4, 15.9). Snout length (29.1% HL) is within the range of *D. rugosa* (24.6–37.7) and *D. pygmaea* (24.6–33.0), but slightly longer than *D. orientalis* (23.2–27.8) and *D. brevis* (28.3, 28.3). Upper jaw length (40.7% HL) is within the range of *D. rugosa* (37.6–52.8) and *D. pygmaea* (39.2–47.1), but slightly shorter than *D. orientalis* (43.9–48.0) and *D. brevis* (43.6, 42.6). Lower jaw length (38.3% HL) is within the range of *D. rugosa* (33.3–49.7) and *D. pygmaea* (33.3–44.1), but slightly shorter than *D. orientalis* (39.0–43.4) and slightly longer than *D. brevis* (38.1, 36.7). Pectoral fin length (22.4% HL) is within the range of *D. rugosa* (13.3–23.3) and *D. orientalis* (16.8–23.4), but slightly longer than *D. pygmaea* (13.6–21.7) and *D. brevis* (21.3, 18.5).

A comparison of the meristic and morphometric data of *Dysommina castanea* with the other described species of *Dysommina* show the distinctiveness of the new species, but none of these data are diagnostic for the taxon. Other data shown in Table 1 are diagnostic. First, the number of preoperculomandibular pores is distinctive. *D. castanea* is the only species in the genus with seven pores, six along the mandible and the seventh behind the rictus of the jaw. All other species of *Dysommina* have just the six along the mandible. The dentary and maxillary dentition is also diagnostic. *D. castanea* has fewer rows of teeth (2–5 dentary, 3–5 maxillary) and fewer enlarged teeth in the inner rows (30–33 dentary, 36–37 maxillary**).** Only *D. pygmaea* approaches these values (5–6 rows of teeth on both dentary and maxilla; 28–30 enlarged dentary teeth, 37–40 enlarged maxillary teeth).

Etymology. The name is derived from the Latin *castaneis*, "chestnut" and refers to the deep brown coloration of this species.

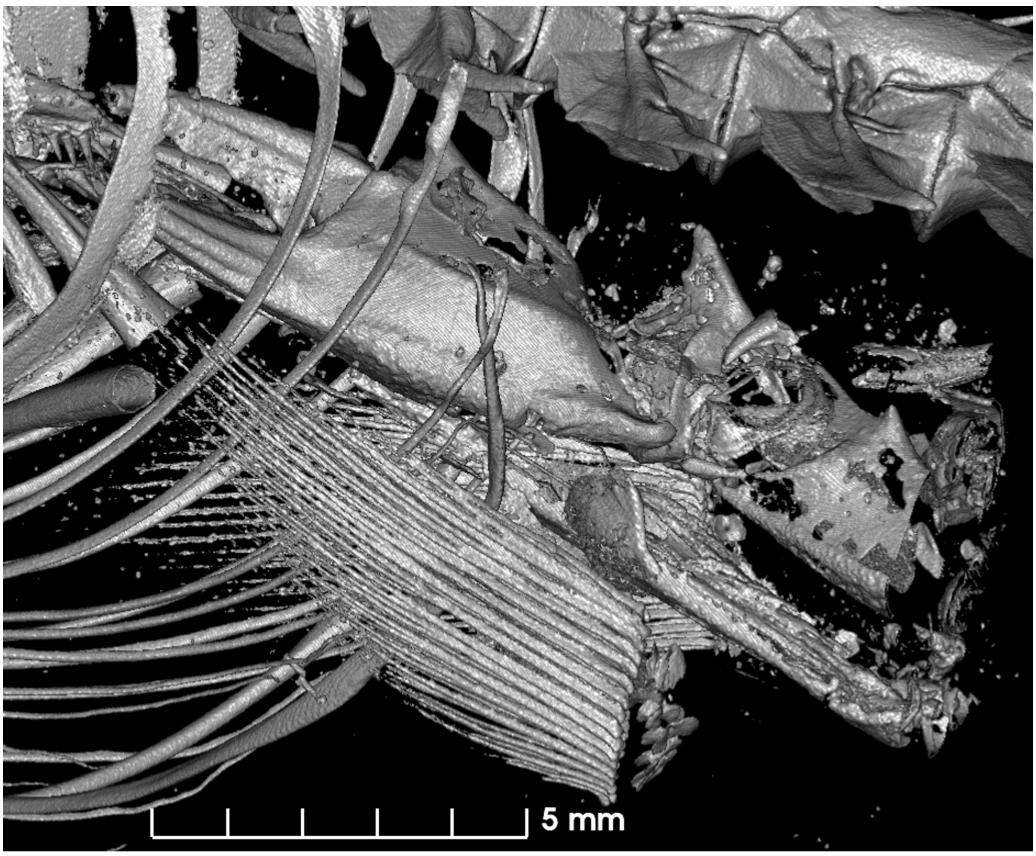

FIGURE 11. MicroCT scan of the foregut of holotype of *Dysommina castanea***,** SAIAB 66023.

Distribution and Ecology. The species is known only from the unique holotype collected on the continental shelf off Angola. However, there is no reason that the species should not be found elsewhere on the shelf off southwestern Africa. There is no information about the bottom type of the area trawled although Tweddle & Anderson (2008) did report that the standard trawl bottom time was usually 30 minutes unless interrupted by hard ground. It is likely that the specimen was collected associated with an area of "hard bottom" since Ross and Quattrini (2007), Ross *et al.* (2015a) and Ross *et al.* (2015b) reported the *Dysommina rugosa* was found primarily in complex, hard-bottomed habitats including rock fields, canyon walls, mixed hard-soft bottom, seeps and deep-water coral reefs. Also, Tighe and Pogonoski (2025) reported that the types of *D. pygmaea* were collected with a beam trawl that was successfully retrieved after a minor hookup on the rocky bottom. It is likely that all species of *Dysommina* inhabit such complex habitats. The holotype did have the claw of a crab in its gut (Fig. 11) indicating *D. castanea* does feed on decapod crustaceans.

Comparative materials. *Dysommina rugosa* (n=73): USNM 131594 (holotype, 196 mm TL), Atlantic Ocean, United States, Georgia, off Cumberland Island, 30°53'00"N, 79°42'30"W, 273 fms (499 m), 5 May 1886. USNM 44324 (1, 283 mm TL), Atlantic Ocean, United States, Georgia, off Savannah, 31°09'00"N, 79°33'30"W, 644 m, 5 May 1886. USNM 179213 (1, 194 mm TL), Gulf of Mexico, off Florida, 28°16'N, 85°50'W, 439 m, 3 Dec 1962. USNM 190541 (1, 265 mm TL), Gulf of Mexico, Florida Keys, southwest of Dry Tortugas, 24°28'N, 83°24'W, 329 m, 7 Jun 1959. USNM 193552 (1, 213 mm TL), Caribbean Sea, off Belize, 16°58'N, 87°53'W, 250–400 fms (457–732 m), 10 Jun 1962. USNM 200776 (1, 248 mm TL), Atlantic Ocean, east coast of Florida, 29°59'N, 80°09'W, 347 m, 21 Nov 1965. USNM 441960 (1, 226 mm TL), USNM 441961 (1, 224 mm TL), Atlantic Ocean, off Maryland, Baltimore Canyon seep, 38°02'53"N, 73°49'19"W, 398 m, 16 May 2013. USNM 441962 (1, 249 mm TL), Atlantic Ocean, off Maryland, Baltimore Canyon seep, 38°02'57.1"N, 73°49'19.6"W, 414 m, 7 Sep 2012. NCSM 115346 (1, 96 mm TL), Atlantic Ocean, off North Carolina, Cape Lookout Lophelia A, ca. 197.3–197.6 kilometers E of Wilmington, 34°19'42"N, 75°47'59"W, 370–407 m, 15 Jun 2004. NCSM 115347 (1, 180 mm TL), Atlantic Ocean, off North Carolina, Cape Lookout Lophelia B, ca. 90.6–91.2 kilometers SE of Beaufort, 34°13'55"N, 75°52'01"W, 419–430 m, 20 Sep 2006. NCSM 115348 (2, 128–157 mm TL), Atlantic Ocean, off North Carolina, Lophelia B site, ca. 75.7 kilometers SE Cape Lookout, 34°10'50"N, 75°53'28"W, 397–450 m, 19 Oct 2005. NCSM 115349 (1, 174 mm TL), Atlantic Ocean, off North Carolina, Cape Lookout Lophelia B, ca. 92.9–93.6 kilometers SE of Beaufort, 34°10'54"N, 75°52'57"W, 458–465 m, 19 Sep 2006. NCSM 115350 (1, 176 mm TL), Atlantic Ocean, off North Carolina, Cape Lookout Lophelia A, ca. 92.4–92.3 kilometers ESE of Beaufort, 34°18'48"N, 75°47'4"W, 389–443 m, 23 Sep 2001. NCSM 115351 (1, 184 mm TL), Atlantic Ocean, off North Carolina, Cape Lookout Lophelia A, ca. 91.2 kilometers ESE of Beaufort, 34°19'25"N, 75°47'30"W, 367–399 m, 22 Sep 2001. NCSM 115352 (4, 80–158 mm TL), Atlantic Ocean, off North Carolina ca. 74.7–75.1 kilometers SE of Cape Lookout, 34°11'12"N, 75°53'49"W, 431 m, 19 Sep 2006. NCSM 115353 (1, 193 mm TL), Atlantic Ocean, off Maryland, Baltimore Canyon, ca. 115.7–117.9 kilometers ESE of Ocean City, 38°02'47"N, 73°49'07"W, 7 Sep 2012. NCSM 115354 (3, 145–217 mm TL), Atlantic Ocean, off North Carolina, Cape Lookout Lophelia B, ca. 92.8–92.9 kilometers SE of Beaufort, 34°10'46"N, 75°53'26"W, 450–487 m, 24 Sep 2001. NCSM 115355 (2, 220–225 mm TL), Atlantic Ocean, off Maryland, Baltimore Canyon, ca. 159.6–159.2 kilometers ESE of Salisbury, 38°02'52"N, 73°49'11"W, 399–443 m, 16 May 2013. NCSM 115356 (1, 210 mm TL), Atlantic Ocean, off North Carolina, Cape Lookout Lophelia A, ca. 90.7–90.3 kilometers ESE of Beaufort, 34°19'06"N, 75°48'13"W, 396–405 m, 10 Aug 2002. NCSM 115357 (15, 166–206 mm TL), Atlantic Ocean, off North Carolina, Cape Lookout Lophelia B, ca. 91.7–92.3 kilometers SE of Beaufort, 34°11'57"N, 75°52'59"W, 423–443 m, 19 Sep 2006. NCSM 115358 (4, 169–237 mm TL), Atlantic Ocean, off North Carolina, Cape Lookout, ca. 91.8–91.7 kilometers ESE of Beaufort, 34°17'38"N, 75°48'19"W, 438–439 m, 5 Dec 2009. ANSP 94286 (1, 155 mm TL), Atlantic Ocean, off St. Augustine, 29°56'N, 80°10'W, M/V Combat Station 84, 190 fms (165 m), 1 Sep 1956. ANSP 102469 (1, 162 mm TL), Atlantic Ocean, Atlantic coast of Florida, 29°53'N, 80°11'W, R/V Silver Bay Station 3677, 180 fms (329 m), 20 January 1962. ANSP 106150 (1, 149 mm TL), Atlantic Ocean, Atlantic coast of Florida, 30°21'N, 79°55'W, 230–250 fms (420–457 m), R/V Atlantis Station 3779, 24 February 1940. ANSP 110079 (1, 337 mm TL), Atlantic Ocean, Atlantic coast of Florida, 92°53'N, 80°11'W, 175–180 fms (320–329 m), R/V Silver Bay Station 3669, 18 January 1962. ANSP 114438 (1, 245 mm TL), Atlantic Ocean, Gulf of Mexico, Straits of Florida, 24°26'N, 83°31'W, 300 fms (549 m), R/V Oregon Station 4373, 7 Aug 1963. ANSP 114439 (1, 218 mm TL), Atlantic Ocean, between Florida and The Bahamas, 26°14'N, 79°30.5'W, 351 fms (642 m), R/V Gerda Station 299, 5 April 1964. ANSP 114440 (1, 173 mm TL), Atlantic Ocean, Straits of Florida, 24°10'N, 81°39'W, 345 fms (631 m), R/V Gerda Station 362, 15 Sep 1964. ANSP 114441 (1, 228

mm TL), Atlantic Ocean, Atlantic coast of Florida, 157–143 fms (287–262 m), R/V Gerda Station 655, 16 Jul 1965. ANSP 114442 (1, 174 mm TL), Atlantic Ocean, Atlantic coast of Florida, 27°08'N, 79°45'W, 220 fms (403 m), R/V Gerda Station 652, 16 Jul 1965. ANSP 114443 (1, 166 mm TL), Atlantic Ocean, Atlantic coast of Florida, 29°55'N, 80°11' W, 180–182 fms (329–333 m), R/V Silver Bay Station 3675, 19 January 1962. ANSP 114444 (1, 338 mm TL), Atlantic Ocean, Atlantic coast of Florida, 29°53'N, 80°11' W, 180 fms (329 m), R/V Silver Bay Station 3680, 21 January 1962. ANSP 114445 (1, 347 mm TL), Atlantic Ocean, Atlantic coast of Florida, 29°42'N, 80°11' W, 170 fms (311 m), R/V Silver Bay Station 3679, 20 January 1962. ANSP 114449 (1, 137 mm TL), Atlantic Ocean, Atlantic coast of Florida, 30°40'N, 79°57'W, 210 fms (384 m), M/V Combat Station 310, 24 April 1957. ANSP 117045 (1, ca. 280 mm TL), Atlantic Ocean, off Florida, 30°2'N, 80°6'W. 215 fms (393 m), R/V Oregon Station 5761, 20 November 1965. ANSP 130216 (1, 268 mm TL), Atlantic Ocean, off coast of North Carolina, 33°56'N, 75°56'W, 340 fms (622 m), R/V Oregon Station 11758, 31 January 1972. ANSP 130217 (1, 175 mm TL), Atlantic Ocean, off Florida, 30°54'N, 79°40'W, 265 fms (485 m), R/V Oregon Station 11715, 21 January 1972. ANSP 130219 (1, 211 mm TL), Atlantic Ocean, off Georgia, 31°2'N, 79°48'W, 140 fms (256 m), R/V Oregon Station 11710, 20 January 1972. ANSP 153725 (1, 269 mm TL), Atlantic Ocean, Straits of Florida, 24°27'N, 83°25'W, 200 fms (366 m), R/V Oregon Station 11166, 17 Aug 1970. FSBC 016323 (1, 303 mm TL), Atlantic Ocean, ca. 39 nautical miles E of Cape Canaveral, 28°40'06"N, 79°45'W, 300 fms (548.6 m), 1 Jun 1984. FSBC 020887 (4, 164–217 mm TL), Atlantic Ocean, ca. 81.5 mi E of Jacksonville, 30°21'06"N, 80°00'24"W, 223 fms (407.8 m), 5 Jun 1985. FSBC 020888 (1, 235 mm TL), Atlantic Ocean, ca. 109 km E of St. Augustine Inlet, 30°05'30"N, 80°09'48"W, 152 fms (278 m), 7 Jun 1985. FSBC 020971 (2, 195–260 mm TL), Atlantic Ocean, ca. 138 km E of southern tip of Amelia Island, 30°31'24"N, 79°59'30"W, 176 fms (321.9 m), 5 Jun 1985. FSBC 021179 (1, 253 mm TL), Atlantic Ocean, ca. 37.5 nautical miles NE of Cape Canaveral, 28°50'18"N, 79°52'12"W, 225 fms (411.5 m), 31 May 1984.

Dysommina orientalis (n=7): NMMB-P11131 (holotype, 413 mm TL), collected from Dong-gang fishing port, Pingtung, Taiwan, 13 Sep. 2010. USNM 441667 (paratype, 316 mm TL; formerly NMMB-P14012), Dong-gang fishing port, Pingtung, Taiwan, 20 Oct. 2011; NMMB-P3847 (paratype, 290 mm TL; formerly THUP 4077), Dong-gang fishing port, Pingtung, Taiwan, 21 Mar. 1979; NMMB-P8361 (paratype, 258 mm TL), Dong-gang fishing port, Pingtung, Taiwan, 16 Mar. 2005; USNM 441750 (paratype, 325 mm TL; formerly NSYSU 3028), Dong-gang fishing port, Pingtung, Taiwan, Jan. 1996; ASIZP 57954 (paratype, 238 mm TL), Dong-sha Island, South China Sea, 17 Aug. 1991; OMNH-P10000 (paratype, 625 mm TL), Suruga Bay, Shizuoka Prefecture, Japan, 34°54'N, 138°30.5'E, 300–400 m depth, 17 Dec. 1996.

Dysommina pygmaea (n=4): NMV A 29681-004 (holotype, 145 mm TL), Australia: Western Australia: Rowley Shoals, Mermaid L34 east transect (17°02'50"S, 119°39'41"E to 17°03'42"S, 119°41'22"E), 424–456 m depth, RV Southern Surveyor, Station SS0507/77, 18 Jun 2007; NMV A 29681-009 (paratype, 169 mm TL, cleared and stained); CSIRO H 6607-01 (paratype, 147 mm TL); USNM 443847 (paratype, 161 mm TL), same data as holotype.

Acknowledgements

The author would like to thank Ofer Gon and the staff of the South African Institute for Aquatic Biodiversity (SAIAB) for making the specimen available. I also thank Teresa Hsu and Jennifer J. Hill for their help with the MicroCT scans, and Matthew G. Girard and Leo MacLeod for their help with 3D Slicer.

References

Böhlke, E.B. (1982) Vertebral formulae for type specimens of eels (Pisces: Anguilliformes). *Proceedings of the Academy of Natural Sciences, Philadelphia*, 134, 31–49.

Böhlke, E.B. (1989) Methods and terminology. *In*: Böhlke, E.B. (Ed.), Fishes of the Western North Atlantic. *Memoir of the Sears Foundation for Marine Research*, 1 (Part 9), pp. 1–7. https://doi.org/10.2307/j.ctvbcd0dm.4

Chen, Y.-Y. & Mok, H.-K. (2001) A new synaphobranchid eel, *Dysomma longirostrum* (Anguilliformes: Synaphobranchidae), from the northeastern coast of Taiwan. *Zoological Studies*, 40 (2), 79–83.

Fedorov, A., Beichel, R., Kalpathy-Cramer, J., Finet, J., Fillion-Robin, J.-C., Pujol, S., Bauer, C., Jennings, D., Fennessy, F., Sonka, M., Buatti, J., Aylward, S., Miller, J.V., Pieper, S. & Kikinis, R. (2012) 3D slicer as an image computing platform for the quantitative imaging network. *Magnetic Resonance Imaging*, 30, 1323–1341.

https://doi.org/10.1016/j.mri.2012.05.001
Ginsburg, I. (1951) The eels of the northern Gulf Coast of the United States and some related species. *Texas Journal of Science*, 3 (3), 431–485.
Haimovici, M., Martins, A.S., Figurredo, J.L. & Viera, P.C. (1994) Demersal bony fish of the outer shelf and upper slope of the southern Brazil Subtropical Convergence Ecosystem. *Marine Ecology Progress Series*, 108, 59–77. https://doi.org/10.3354/meps108059
Hatooka, K. (1997) First record of the deep-sea eel, *Dysommina rugosa* from Suruga Bay, Central Japan (Pisces: Synaphobranchidae). *Bulletin of the Osaka Museum of Natural History*, 51, 7–12.
Ho, H.-C., Smith, D.G. & Tighe, K.A. (2015) Review of the arrowtooth eel genera *Dysomma* and *Dysommina* in Taiwan, with the description of a new species (Anguilliformes: Synaphobranchidae: Ilyophinae). *Zootaxa*, 4060 (1), 86–104. https://doi.org/10.11646/zootaxa.4060.1.12
Karrer, C. (1983) Anguilliformes du Canal de Mozambique (Pisces, Teleostei). *Faune Tropicale*, 23, 1–116.
Robins, C.H. & Robins, C.R. (1970) The eel family Dysommidae (including the Dysomminidae and Nettodaridae), its osteology and composition, including a new genus and species. *Proceedings of the Academy of Natural Sciences, Philadelphia*, 122 (6), 293–335.
Robins, C.H. & Robins, C.R. (1976) New genera and species of dysommine and synaphobranchine eels (Synaphobranchidae) with an analysis of the Dysomminae. *Proceedings of the Academy of Natural Sciences, Philadelphia*, 127 (18), 249–280.
Robins, C.H. & Robins, C.R. (1989) Family Synaphobranchidae. *In*: Böhlke, E.B. (Ed.), Fishes of the Western North Atlantic. *Memoir of the Sears Foundation for Marine Research*, 1 (Part 9), pp. 207–253. https://doi.org/10.2307/j.ctvbcd0dm.12
Sabaj, M.H. (2020) Codes for Natural History Collections in Ichthyology and Herpetology. Copeia, 108 (3), 593–669. https://doi.org/10.1643/ASIHCODONS2020
Sabaj, M.H. (2025) Codes for Natural History Collections in Ichthyology and Herpetology (online supplement). Version 9.7. 3 March 2025. American Society of Ichthyologists and Herpetologists, Washington, D.C. Available from: https://www.asih.org/resources/standard-symbolic-codes (accessed 1 May 2025)
Saruwatari, T., López, J.A. & Pietsch, T.W. (1997) Cyanine Blue: a versatile and harmless stain for specimen observation. *Copeia*, 1997 (4), 840–841. https://doi.org/10.2307/1447302
Staudigel, H., Hart, S.R., Pile, A., Bialey, B.E., Baker, E.T., Brooke, S., Connelly, D.P., Haucke, L., German, C.R., Hudson, I., Jones, D., Koopers, A.A.P., Konter, J., Lee, R., Pietsch, T.W., Tebo, B.M., Templeton, A.S., Zierenberg, R. & Young, C.M. (2006) Vailulu'u Seamount, Samoa: Life and death on an active submarine volcano. *Proceedings of the National Academy of Sciences*, 103 (17), 6448–6453. https://doi.org/10.1073/pnas.0600830103
Tighe, K.A., Ho, H.-C. & Hatooka, K. (2018) A new species of the genus *Dysommina* (Teleostei: Anguilliformes: Synaphobranchidae: Ilyophinae) from the Western Pacific. *Zootaxa*, 4454 (1), 43–51. https://doi.org/10.11646/zootaxa.4454.1.6
Tighe, K.A. & Pogonoski, J.J. (2025) A new species of the genus *Dysommina* (Teleostei: Anguilliformes: Synaphobranchidae: Ilyophinae) from the eastern Indian Ocean. *Zootaxa*, 5683 (2), 265–281. https://doi.org/10.11646/zootaxa.5683.2.6
Tweddle, D. & Anderson, M.E. (2008) A collection of marine fishes from Angola, with notes on new distribution records. *Smithiana Bulletin*, 8, 3–24.
Uyeno, T. & Sasaki, K. (1983) *Dysommina rugosa* Ginsburg, 1951. *In*: Uyeno, T., Matsubara, T. & Fuji, E. (Eds.), *Fishes trawled off Surinam and French Guiana*. Japan Marine Fishery Resource Research Center, Tokyo, pp. 107.
Vo, Q.V., Ho, H.-C., Dao, H.V. & Tran, T.C. (2024) New species of the eel genera *Dysomma* and *Dysommina* from Vietnam, South China Sea (Anguilliformes: Synaphobranchidae). *Journal of Fish Biology*, 104 (4), 1067–1078. https://doi.org/10.1111/jfb.15638